IOP Publishing Physica Scripta
Phys. Scr. 95 (2020) 035207 (12pp) https://doi.org/10.1088/1402-4896/ab4a50

Instability modulation for the (2+1)-dimension paraxial wave equation and its new optical soliton solutions in Kerr media

Wei Gao[1,2], Hajar F Ismael[3,4], Hasan Bulut[4] and Haci Mehmet Baskonus[1,5]

[1] Department of Mathematics and Science Education, Harran University, Sanliurfa, Turkey
[2] School of Information Science and Technology, Yunnan Normal University, Kunming 650500, People's Republic of China
[3] Department of Mathematics, Faculty of Science, University of Zakho, Zakho, Iraq
[4] Department of Mathematics, Faculty of Science, Firat University, Elazig, Turkey

E-mail: gaowei@ynnu.edu.cn and hmbaskonus@gmail.com

Received 17 August 2019, revised 19 September 2019
Accepted for publication 2 October 2019
Published 3 February 2020

Abstract

In this paper, we use the modified auxiliary expansion method to seek some new solutions of the paraxial nonlinear Schrödinger equation. The solutions have a hyperbolic function, trigonometric function, exponential function, and rational function forms The linear stability analysis of paraxial NLSE is also presented to study the modulational instability (MI). Two cases when the instability modulation becomes to occur are investigated. Depending on MI cases, the MI gain spectrum are also investigated and presented graphically. All solutions are new and verified the main equation of the paraxial wave equation. Moreover, the constraint conditions for the existence of soliton solutions are also showed.

Keywords: instability modulation, praxial wave equation, modified auxiliary expansion method

(Some figures may appear in colour only in the online journal)

1. Introduction

The dispersal of ultrashort pulses of electromagnetic radiation into a nonlinear medium is a multidimensional phenomenon. The interaction between different physical procedures such as dispersion, material dispersion, diffraction, and nonlinear response impacts the pulse dynamics. Due to the interaction of dispersion, diffraction and nonlinearity, a non-dispersive and non-diffractive wave packet called soliton (light bullet) is created. Solitons have many applications in optical microscopy, optical information storage, laser-induced particle acceleration, Bose–Einstein condensation, and high-resolution signal transmission [1].

The ubiquitous phenomenon that originates from the interplay of linear dispersion or diffraction and the nonlinear self-interaction of wave areas is called modulational instability (MI). This impact was first theoretically recognized by Benjamin and Feir in 1967 for deep-water waves [2]. MI studies are increasingly interested in nonlinear optics, fluid dynamics, Bose–Einstein condensate, physics of plasma and other areas.

Many methods are used to find and analyze solutions of nonlinear differential equations, such as shooting with Runga–Kutta fourth-order technique [3–6], finite difference method [7, 8], homotopy perturbation method [9], Adams–Bashforth–Moulton method [10], Adomian decomposition method [11], trial equation method [12], the modified Darboux transformation technique [13], the Bäcklund transformations method [14], the simple equation method [15], sine-Gordon expansion method [16], lie symmetries along with (G'/G) expansion method [17], the the bilinear method [18, 19], extended trial equation method [20], the extended sinh-Gordon expansion method [21–23], improved Bernoulli sub-equation function method [24, 25], the multiplier approach [26], modified simple equation method [27], exp $(-\varphi(\xi))$ expansion method [28], method of undetermined coefficients [29], couple of integration schemes [30], improved tan $(\phi(\xi)/2)$-expansion method [31], tanh function

[5] Author to whom any correspondence should be addressed.

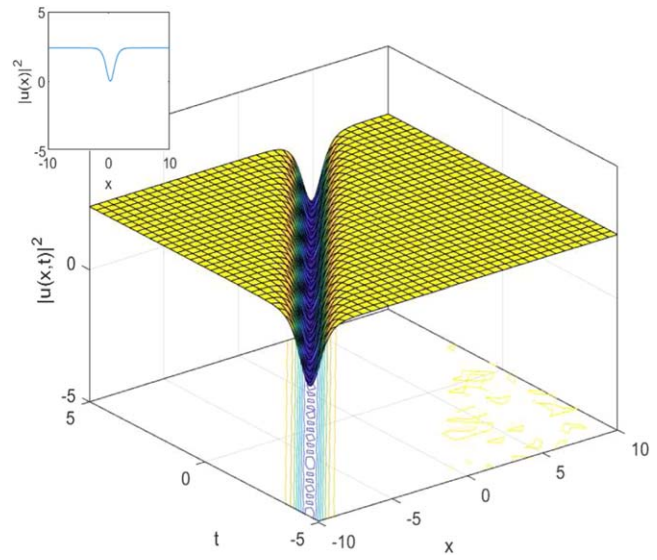

Figure 1. 3D and contour plot of equation (13) when $\lambda = 3$, $\mu = 1$, $\omega = -1$, $\epsilon = 1$, $\kappa = 2$, $y = 1$, $\nu = 1$ and $\gamma = 2$.

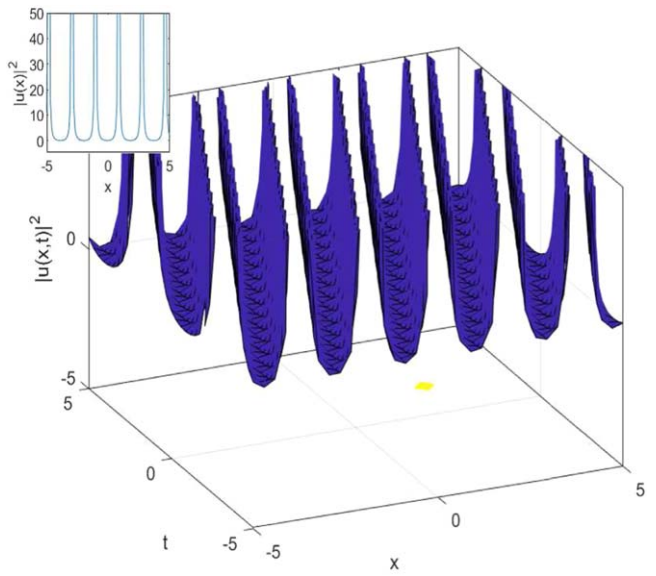

Figure 2. 3D and contour plot of equation (14) when $\lambda = 1$, $\mu = 3$, $\omega = -1$, $\epsilon = 1$, $\kappa = 2$, $y = 1$, $\nu = 3$ and $\gamma = 2$.

method [32], the modified tanh-function method [33], Jacobi elliptic function anzätz method [34], the modified kudryashov method [35], and inverse mapping method [36]. In [37], authors extended the variable coefficient Jacobian elliptic function method to solve nonlinear differential equation. The balance between different-order nonlinearities and high-order dispersion/diffraction in parity-time symmetric potentials was used to construct three-dimensional optical solitons [38]. In [39, 40], exact vector multipole and vortex solitons of nonlinear Schrödinger equation were also investigated. Moreover, many powerful methods have been used and also extended to find new properties of mathematical models symbolizing serious real world problems [41–49].

In this paper, we use the modified auxiliary expansion method to seek novel soliton solutions of the paraxial nonlinear Schrödinger equation. The new solutions are presented in terms of the family solution and expressed in hyperbolic, trigonometric and exponential functions. Finally, the instability modulation of the paraxial wave equation is also presented.

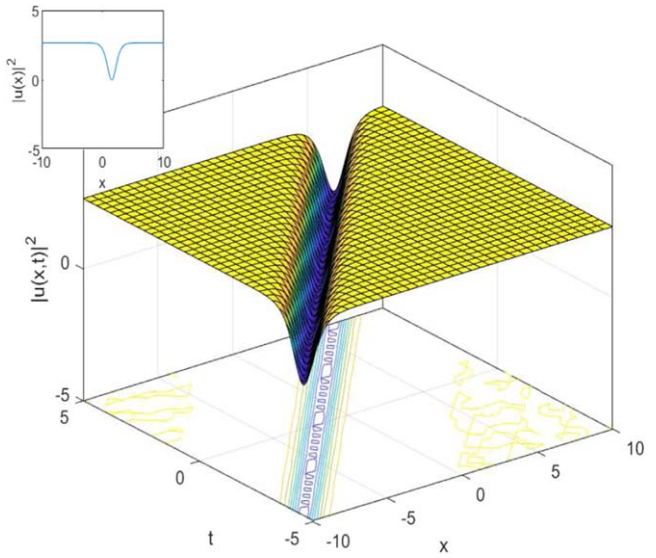

Figure 3. 3D and contour plot of equation (15) when $\lambda = 0$, $\mu = -1$, $\omega = -1$, $\epsilon = 1$, $\kappa = 2$, $y = 1$, $\nu = 1$ and $\gamma = 2$.

2. General form of methods

Suppose that, we have the following nonlinear partial differential equation

$$P(u, u_x, u^2u_x, u_t, u_{tt},\ldots) = 0. \tag{1}$$

To find the explicit exact solutions of equation (1), we use the following transformation

$$u(x, y, t) = U(\xi), \quad \xi = x - \nu\, t, \tag{2}$$

where ν is arbitrary constant and ξ is the symbol of the wave variable. Substituting equation (2) to equation (1), the result is a nonlinear ordinary differential equation as follows

$$N(U, U^2, U', U'',\ldots) = 0. \tag{3}$$

Now the trial equation of solution for equation (3) is defined as

$$U(\xi) = a_0 + \sum_{i=1}^{n} a_i K^{i\,\Phi(\xi)} + \sum_{i=1}^{n} b_i K^{-i\,\Phi(\xi)}, \tag{4}$$

where a_i and b_i, $(1 \leqslant i \leqslant n)$ are non-zero constants and $\Phi(\xi)$

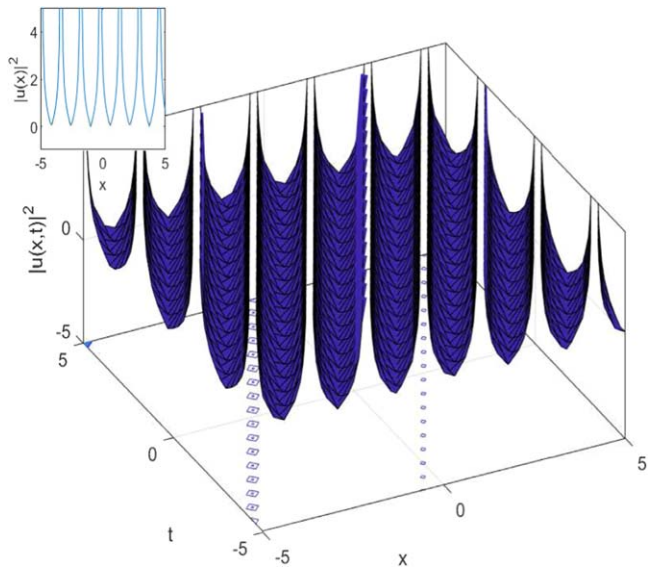

Figure 4. 3D and contour plot of equation (16) when $\lambda = 0$, $\mu = 4$, $\omega = -1$, $\epsilon = 1$, $\kappa = 2$, $y = 1$, $\nu = 1$ and $\gamma = 2$.

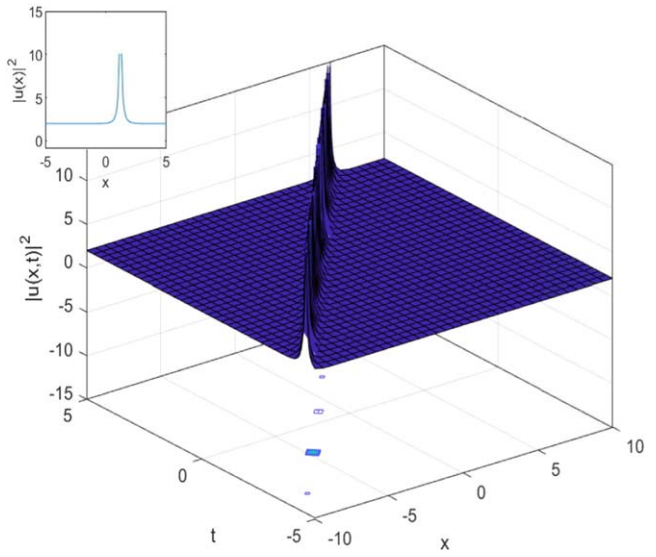

Figure 5. 3D and contour plot of equation (17) when $\lambda = 4$, $\mu = 0$, $\omega = -4$, $\epsilon = 0.2$, $\kappa = 2$, $y = 2$, $\nu = 2$ and $\gamma = 2$.

is the auxiliary ODE given by

$$\Phi'(\xi) = \frac{K^{-\Phi(\xi)} + \mu K^{\Phi(\xi)} + \lambda}{\ln(K)}, \tag{5}$$

where μ, λ are constants and $K > 0$, $K \neq 1$. The auxiliary ODE has the general solution as follows:

(i) When $\lambda^2 - 4\mu > 0$, then $f(\xi) = \log_K \left(-\lambda - \sqrt{\lambda^2 - 4\mu}\tanh\left(\frac{1}{2}\sqrt{\lambda^2 - 4\mu}(C + \xi)\right)\right)$.

(ii) When $\lambda^2 - 4\mu < 0$, then $f(\xi) = \log_K \left(-\lambda + \sqrt{-\lambda^2 + 4\mu}\tan\left(\frac{1}{2}\sqrt{-\lambda^2 + 4\mu}(C + \xi)\right)\right)$.

(iii) When $\lambda^2 - 4\mu \neq 0$, $\lambda = 0$ and $\mu < 0$, then $f(\xi) = \log_K \left(\sqrt{-4\mu}\coth\left(\frac{1}{2}\sqrt{-4\mu}(C + \xi)\right)\right)$.

(iv) When $\lambda^2 - 4\mu \neq 0$, $\lambda = 0$ and $\mu > 0$, then $f(\xi) = \log_K \left(\sqrt{4\mu}\cot\left(\frac{1}{2}\sqrt{4\mu}(C + \xi)\right)\right)$.

(v) When $\lambda^2 - 4\mu > 0$ and $\mu = 0$, then $f(\xi) = \log_K \left(\frac{\lambda}{-1 + \cosh(\lambda(\epsilon + \xi)) + \sinh(\lambda(\epsilon + \xi))}\right)$.

(vi) When $\lambda^2 - 4\mu = 0$, $\lambda \neq 0$ and $\mu \neq 0$, then $f(\xi) = \log_K \left(-\frac{2\lambda(\xi + \epsilon) + 4}{\lambda^2(\xi + \epsilon)}\right)$.

(vii) When $\lambda^2 - 4\mu = 0$, $\lambda = 0$ and $\mu = 0$, then $f(\xi) = \log_K(\xi + \epsilon)$.

The paraxial NLSE in Kerr media is given by

$$\mathrm{i}u_y + \frac{\alpha}{2}u_{tt} + \frac{\beta}{2}u_{xx} + \gamma|u|^2 u = 0, \tag{6}$$

where $u = u(x, y, t)$ is the complex wave envelope function. The constants α , β and γ are the symbols of the dispersion, diffraction and Kerr nonlinearity, respectively. In equation (1) if we get elliptic nonlinear Schrödinger equation and if $\alpha\beta < 0$, equation (1) becomes hyperbolic nonlinear Schrödinger equation. Now assume the following wave transformations:

$$u(x, y, t) = U(\xi)\mathrm{e}^{\mathrm{i}\theta}, \quad \xi = x + y - ct, \quad \theta = \kappa x + \omega y - \nu t, \tag{7}$$

Inserting equation (7) into equation (6), and separate the result into the real and imaginary part, we get

$$-(c^2\alpha + \beta)U'' + (\beta\kappa^2 + \alpha\nu^2 + 2\omega)U - 2\gamma U^3 = 0 \tag{8}$$

and

$$(1 + \beta\kappa + c\alpha\nu)U' = 0. \tag{9}$$

Now, we know that $U' \neq 0$, therefore

$$\beta = \frac{-1 - c\alpha\nu}{\kappa}. \tag{10}$$

Putting equation (10) into equation (8) to get the closed solution, we get

$$(1 - c^2\alpha\kappa + c\alpha\nu)U'' - \kappa(\kappa + c\alpha\kappa\nu - \alpha\nu^2 - 2\omega)U - 2\gamma\kappa U^3 = 0. \tag{11}$$

Finding the homogeneous principal balance between U'' and U^3, we get $n = 1$. Putting the value of into equation (4), the equation (4) can be written as the following

$$U(\xi) = a_0 + a_1 K^{\phi(\xi)} + b_1 K^{-\phi(\xi)}. \tag{12}$$

Using equation (12) and its second derivative with equation (11), we analyze the following cases and solutions:

Case 1. When $a_0 = \frac{\mathrm{i}\lambda\sqrt{\kappa - 2\omega}\sqrt{2\kappa^3 + 3\kappa(\lambda^2 - 4\mu) - 4\kappa^2\omega - 2(\lambda^2 - 4\mu)\omega}}{2\sqrt{\gamma(\lambda^2 - 4\mu)^2(\kappa - \omega)}}$, $b_1 = \frac{\mathrm{i}\sqrt{\kappa - 2\omega}\sqrt{2\kappa^3 + 3\kappa(\lambda^2 - 4\mu) - 4\kappa^2\omega - 2(\lambda^2 - 4\mu)\omega}}{\sqrt{\gamma(\lambda^2 - 4\mu)^2(\kappa - \omega)}}$, $a_1 = 0$, $c = \nu\left(\frac{1}{\kappa} + \frac{2\kappa}{\lambda^2 - 4\mu} + \frac{1}{\kappa - 2\omega}\right)$ and $\alpha = \frac{(\kappa - 2\omega)^2}{2\nu^2(\kappa - \omega)}$ we get the following family solution:

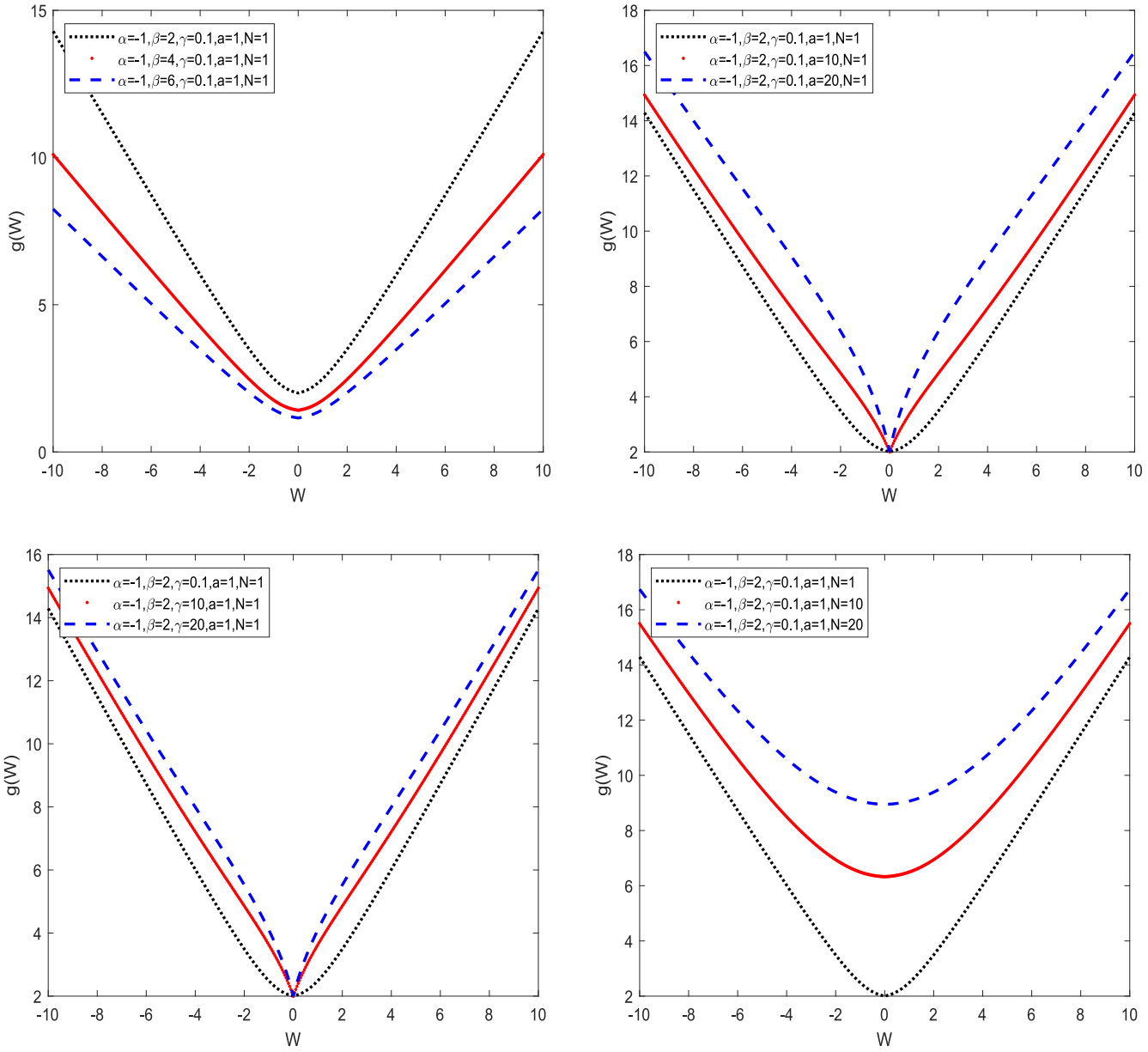

Figure 6. The MI gain spectra in the normal-GVD regime ($\alpha = -1$) for different values mentioned at legends for equation (45).

Family 1. When $\lambda^2 - 4\mu > 0$, $\lambda \neq 0$, $\mu \neq 0$ and $\gamma > 0$, then

$$u(x, y, t) = \frac{\mathrm{i}e^{\mathrm{i}(x\kappa - t\nu + y\omega)}\sqrt{\kappa - 2\omega}\sqrt{2\kappa^3 + 3\kappa(\lambda^2 - 4\mu) - 4\kappa^2\omega - 2(\lambda^2 - 4\mu)\omega}}{2\sqrt{\gamma(\lambda^2 - 4\mu)^2(\kappa - \omega)}}$$
$$\left(\frac{\lambda^2 - 4\mu + \lambda\sqrt{\lambda^2 - 4\mu}\tanh\left(\frac{1}{2}\sqrt{\lambda^2 - 4\mu}\left(x + y + \epsilon - t\nu\left(\frac{1}{\kappa} + \frac{2\kappa}{\lambda^2 - 4\mu} + \frac{1}{\kappa - 2\omega}\right)\right)\right)}{\left(\lambda + \sqrt{\lambda^2 - 4\mu}\tanh\left(\frac{1}{2}\sqrt{\lambda^2 - 4\mu}\left(x + y + \epsilon - t\nu\left(\frac{1}{\kappa} + \frac{2\kappa}{\lambda^2 - 4\mu} + \frac{1}{\kappa - 2\omega}\right)\right)\right)\right)}\right), \tag{13}$$

which is dark soliton solution of equation (6).

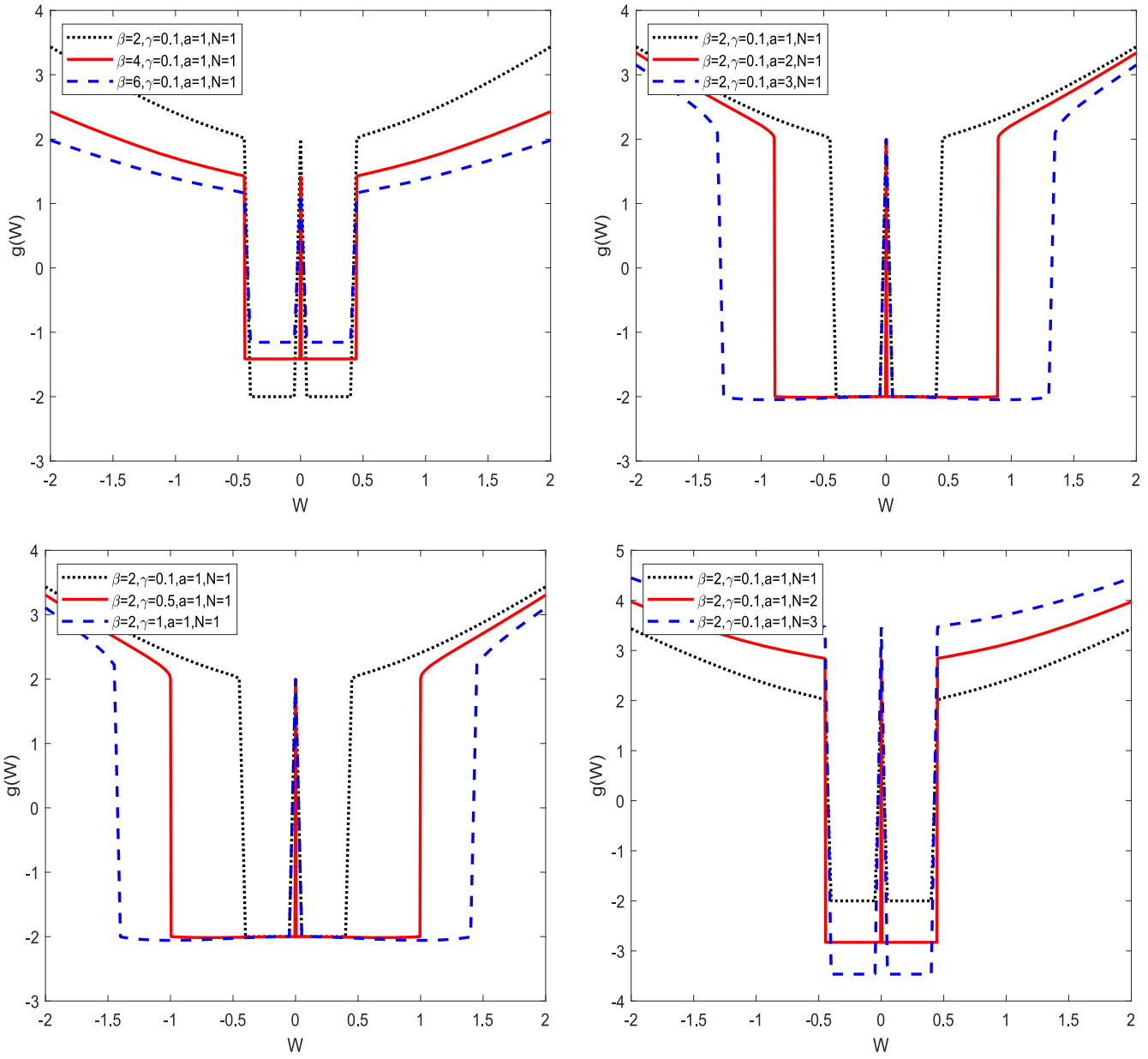

Figure 7. The MI gain spectra in the anomalous-GVD regime ($\alpha = 1$) for different values mentioned at legends for equation (45).

Family 2. When $\lambda^2 - 4\mu < 0$, $\lambda \neq 0$, $\mu \neq 0$ and $\gamma < 0$, then

$$u(x, y, t) = \frac{\mathrm{i}e^{\mathrm{i}(x\kappa - t\nu + y\omega)}\sqrt{\kappa - 2\omega}\sqrt{2\kappa^3 + 3\kappa(\lambda^2 - 4\mu) - 4\kappa^2\omega - 2(\lambda^2 - 4\mu)\omega}}{2\sqrt{\gamma(\lambda^2 - 4\mu)^2(\kappa - \omega)}}$$
$$\left(\lambda - \frac{4\mu}{\lambda - \sqrt{-\lambda^2 + 4\mu}\tan\left[\frac{1}{2}\sqrt{-\lambda^2 + 4\mu}\left(x + y + \epsilon - t\nu\left(\frac{1}{\kappa} + \frac{2\kappa}{\lambda^2 - 4\mu} + \frac{1}{\kappa - 2\omega}\right)\right)\right]}\right), \tag{14}$$

which is singular solution of equation (6).

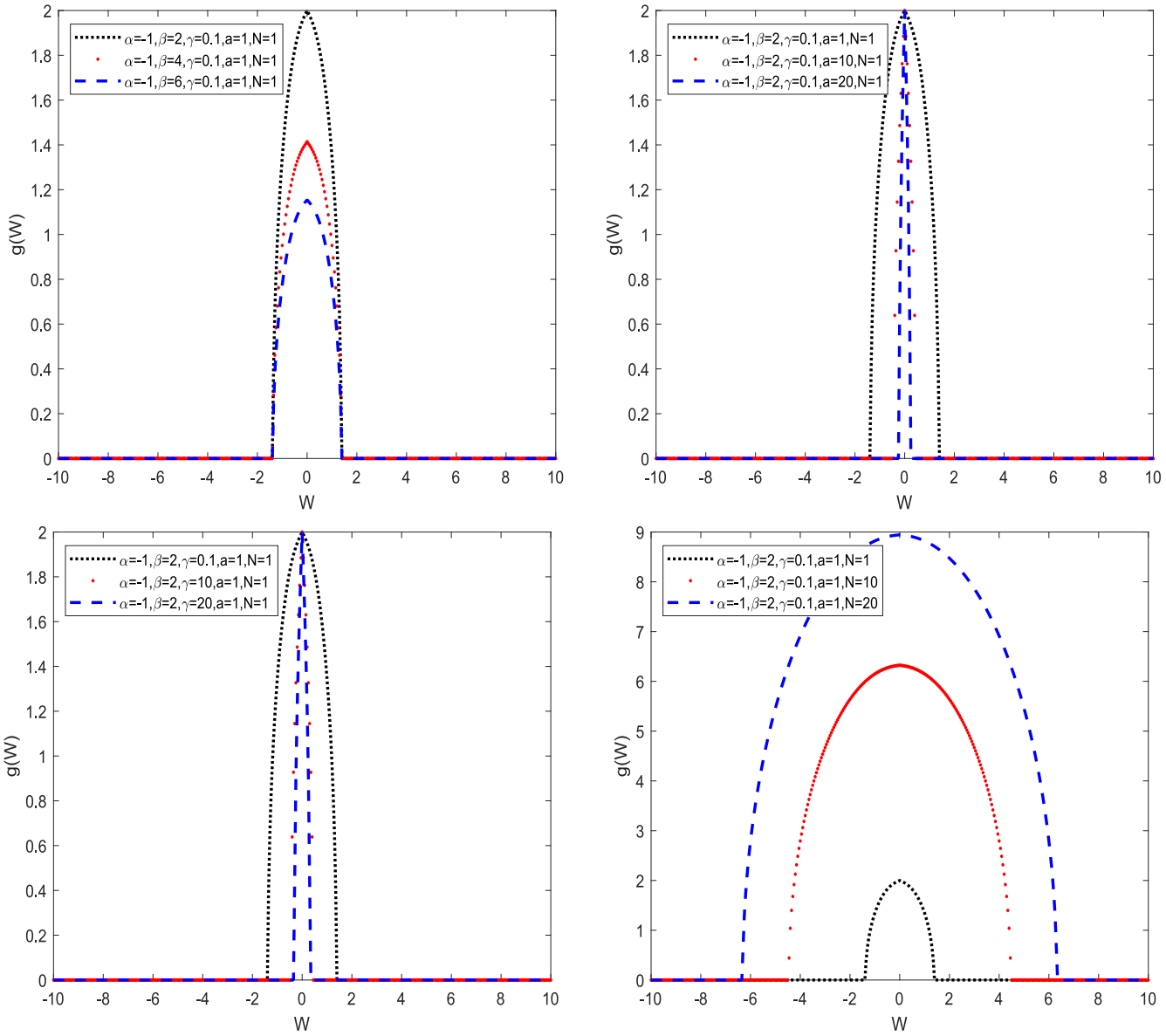

Figure 8. The MI gain spectra in the normal-GVD regime ($\alpha = -1$) for different values mentioned at legends for equation (46).

Family 3.When $\lambda = 0$, $\mu < 0$ and $\gamma > 0$, then

$$u(x, y, t) = \frac{\mathrm{i}e^{\mathrm{i}(x\kappa - t\nu + y\omega)}\sqrt{-\mu}\sqrt{\kappa - 2\omega}\sqrt{2\kappa^3 - 12\kappa\mu - 4\kappa^2\omega + 8\mu\omega}}{4\sqrt{\gamma\mu^2(\kappa - \omega)}}$$
$$\tanh\left(\sqrt{-\mu}\left(x + y + \epsilon - t\nu\left(\frac{1}{\kappa} - \frac{\kappa}{2\mu} + \frac{1}{\kappa - 2\omega}\right)\right)\right), \tag{15}$$

which is dark soliton solution of equation (6).

Family 4. When $\lambda = 0$, $\mu > 0$ and $\gamma < 0$, then

$$u(x, y, t) = \frac{\mathrm{i}e^{\mathrm{i}(x\kappa - t\nu + y\omega)}\sqrt{\mu}\sqrt{\kappa - 2\omega}\sqrt{2\kappa^3 - 12\kappa\mu - 4\kappa^2\omega + 8\mu\omega}}{4\sqrt{\gamma\mu^2(\kappa - \omega)}}$$
$$\tan\left(\sqrt{\mu}\left(x + y + \epsilon - t\nu\left(\frac{1}{\kappa} - \frac{\kappa}{2\mu} + \frac{1}{\kappa - 2\omega}\right)\right)\right), \tag{16}$$

which is singular solution of equation (6).

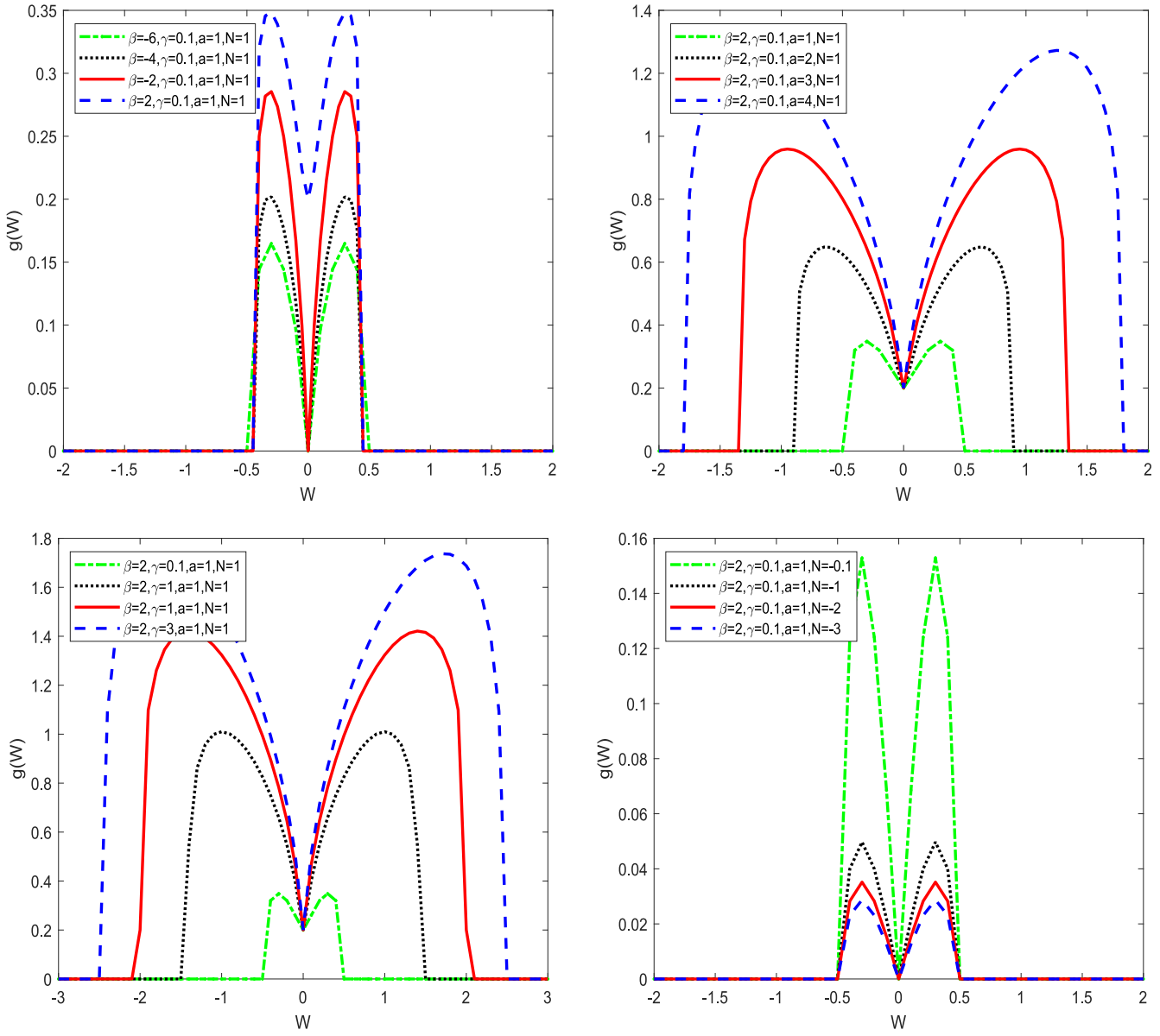

Figure 9. The MI gain spectra in the anomalous-GVD regime ($\alpha = 1$) for different values mentioned at legends for equation (46).

Family 5. When $\lambda^2 - 4\mu > 0$, $\mu = 0$ and $\gamma > 0$, then

$$u(x, y, t) = \frac{\mathrm{i}e^{\mathrm{i}(x\kappa - t\nu + y\omega)}\lambda\sqrt{\kappa - 2\omega}\sqrt{2\kappa^3 + 3\kappa\lambda^2 - 4\kappa^2\omega - 2\lambda^2\omega}\coth\left(\frac{1}{2}\lambda\left(x + y + \epsilon - t\nu\left(\frac{1}{\kappa} + \frac{2\kappa}{\lambda^2} + \frac{1}{\kappa - 2\omega}\right)\right)\right)}{2\sqrt{\gamma\lambda^4(\kappa - \omega)}}, \quad (17)$$

which is singular solution of equation (6).

Case 2. When $a_0 = \frac{\mathrm{i}\lambda\sqrt{\kappa - 2\omega}\sqrt{2\kappa^3 + 3\kappa(\lambda^2 - 4\mu) - 4\kappa^2\omega - 2(\lambda^2 - 4\mu)\omega}}{2\sqrt{\gamma(\lambda^2 - 4\mu)^2(\kappa - \omega)}}$, $a_1 = \frac{\mathrm{i}\mu\sqrt{\kappa - 2\omega}\sqrt{2\kappa^3 + 3\kappa(\lambda^2 - 4\mu) - 4\kappa^2\omega - 2(\lambda^2 - 4\mu)\omega}}{\sqrt{\gamma(\lambda^2 - 4\mu)^2(\kappa - \omega)}}$, $b_1 = 0$, $c = \nu\left(\frac{1}{\kappa} + \frac{2\kappa}{\lambda^2 - 4\mu} + \frac{1}{\kappa - 2\omega}\right)$ and $\alpha = \frac{(\kappa - 2\omega)^2}{2\nu^2(\kappa - \omega)}$ we get the following family solution:

Family 1. When $\lambda^2 - 4\mu > 0$, $\lambda \neq 0$, $\mu \neq 0$ and $\gamma > 0$, then

$$u(x, y, t) = -\frac{\mathrm{i}e^{\mathrm{i}(x\kappa - t\nu + y\omega)}\sqrt{\lambda^2 - 4\mu}\sqrt{\kappa - 2\omega}\sqrt{2\kappa^3 + 3\kappa(\lambda^2 - 4\mu) - 4\kappa^2\omega - 2(\lambda^2 - 4\mu)\omega}}{2\sqrt{\gamma(\lambda^2 - 4\mu)^2(\kappa - \omega)}}$$
$$\tanh\left(\frac{1}{2}\sqrt{\lambda^2 - 4\mu}\left(x + y + \epsilon - t\nu\left(\frac{1}{\kappa} + \frac{2\kappa}{\lambda^2 - 4\mu} + \frac{1}{\kappa - 2\omega}\right)\right)\right). \tag{18}$$

Family 2. When $\lambda^2 - 4\mu < 0$, $\lambda \neq 0$, $\mu \neq 0$ and $\gamma > 0$, then

$$u(x, y, t) = \frac{\mathrm{i}e^{\mathrm{i}(x\kappa - t\nu + y\omega)}\sqrt{\kappa - 2\omega}\sqrt{2\kappa^3 + 3\kappa(\lambda^2 - 4\mu) - 4\kappa^2\omega - 2(\lambda^2 - 4\mu)\omega}}{2\sqrt{\gamma(\lambda^2 - 4\mu)^2(\kappa - \omega)}}$$
$$\left(\lambda - \frac{4\mu}{\lambda - \sqrt{-\lambda^2 + 4\mu}\tan\left(\frac{1}{2}\sqrt{-\lambda^2 + 4\mu}\left(x + y + \epsilon - t\nu\left(\frac{1}{\kappa} + \frac{2\kappa}{\lambda^2 - 4\mu} + \frac{1}{\kappa - 2\omega}\right)\right)\right)}\right). \tag{19}$$

Family 3. When $\lambda = 0$, $\mu < 0$ and $\gamma > 0$, then

$$u(x, y, t) = \frac{\mathrm{i}e^{\mathrm{i}(x\kappa - t\nu + y\omega)}\sqrt{-\mu}\sqrt{\kappa - 2\omega}\sqrt{2\kappa^3 - 12\kappa\mu - 4\kappa^2\omega + 8\mu\omega}}{4\sqrt{\gamma\mu^2(\kappa - \omega)}}$$
$$\tanh\left(\sqrt{-\mu}\left(x + y + \epsilon - t\nu\left(\frac{1}{\kappa} - \frac{\kappa}{2\mu} + \frac{1}{\kappa - 2\omega}\right)\right)\right). \tag{20}$$

Family 4. When $\lambda = 0$ and $\mu > 0$, then

$$u(x, y, t) = \frac{\mathrm{i}e^{\mathrm{i}(x\kappa - t\nu + y\omega)}\sqrt{\mu}\sqrt{\kappa - 2\omega}\sqrt{2\kappa^3 - 12\kappa\mu - 4\kappa^2\omega + 8\mu\omega}}{4\sqrt{\gamma\mu^2(\kappa - \omega)}}$$
$$\tan\left(\sqrt{\mu}\left(x + y + \epsilon - t\nu\left(\frac{1}{\kappa} - \frac{\kappa}{2\mu} + \frac{1}{\kappa - 2\omega}\right)\right)\right). \tag{21}$$

Family 5. $\lambda^2 - 4\mu > 0$ and $\mu = 0$. then

$$u(x, y, t) = \frac{\mathrm{i}e^{\mathrm{i}(x\kappa - t\nu + y\omega)}\lambda\sqrt{\kappa - 2\omega}\sqrt{2\kappa^3 + 3\kappa\lambda^2 - 4\kappa^2\omega - 2\lambda^2\omega}\coth\left(\frac{1}{2}\lambda\left(x + y + \epsilon - t\nu\left(\frac{1}{\kappa} + \frac{2\kappa}{\lambda^2} + \frac{1}{\kappa - 2\omega}\right)\right)\right)}{2\sqrt{\gamma\lambda^4(\kappa - \omega)}}. \tag{22}$$

Case 3. When $a_0 = -\frac{\mathrm{i}\lambda\sqrt{c\kappa + \nu - 2c\omega}}{\sqrt{2c\gamma\lambda^2 - 8c\gamma\mu - 4\gamma\kappa\nu}}$, $a_1 = -\frac{2\mathrm{i}\mu\sqrt{c\kappa + \nu - 2c\omega}}{\sqrt{2c\gamma\lambda^2 - 8c\gamma\mu - 4\gamma\kappa\nu}}$,$b_1 = 0$ and $\alpha = \frac{\lambda^2 - 4\mu + 2\kappa(\kappa - 2\omega)}{(c\kappa - \nu)(c(\lambda^2 - 4\mu) - 2\kappa\nu)}$, we get the following family solutions:

Family 1. When $\lambda^2 - 4\mu > 0$, $\lambda \neq 0$ and $\mu \neq 0$, then

$$u(x, y, t) = \frac{\mathrm{i}e^{\mathrm{i}(x\kappa - t\nu + y\omega)}\sqrt{\lambda^2 - 4\mu}\sqrt{\nu + c(\kappa - 2\omega)}\tanh\left(\frac{1}{2}(-ct + x + y + \epsilon)\sqrt{\lambda^2 - 4\mu}\right)}{\sqrt{2}\sqrt{\gamma(c(\lambda^2 - 4\mu) - 2\kappa\nu)}}. \tag{23}$$

Family 2. When $\lambda^2 - 4\mu < 0$, $\lambda \neq 0$ and $\mu \neq 0$, then

$$u(x, y, t) = -\frac{\mathrm{i}e^{\mathrm{i}(x\kappa - t\nu + y\omega)}\sqrt{-\frac{\lambda^2}{2} + 2\mu}\sqrt{\nu + c(\kappa - 2\omega)}\tan\left(\frac{1}{2}(-ct + x + y + \epsilon)\sqrt{-\lambda^2 + 4\mu}\right)}{\sqrt{\gamma(c(\lambda^2 - 4\mu) - 2\kappa\nu)}}. \tag{24}$$

Family 3. When $\lambda = 0$ and $\mu < 0$, then

$$u(x, y, t) = \frac{\mathrm{i}e^{\mathrm{i}(x\kappa - t\nu + y\omega)}\sqrt{-\mu}\sqrt{\nu + c(\kappa - 2\omega)}\coth((-ct + x + y + \epsilon)\sqrt{-\mu})}{\sqrt{-\gamma(2c\mu + \kappa\nu)}}. \tag{25}$$

Family 4. When $\lambda = 0$ and $\mu > 0$, then

$$u(x, y, t) = -\frac{\mathrm{i}e^{\mathrm{i}(x\kappa - t\nu + y\omega)}\sqrt{\mu}\sqrt{\nu + c(\kappa - 2\omega)}\cot[(-ct + x + y + \epsilon)\sqrt{\mu}]}{\sqrt{-\gamma(2c\mu + \kappa\nu)}}. \tag{26}$$

Family 5. When $\lambda^2 - 4\mu > 0$ and $\mu = 0$, then

$$u(x, y, t) = -\frac{\mathrm{i}\lambda\sqrt{c\kappa + \nu - 2c\omega}}{\sqrt{2c\gamma\lambda^2 - 4\gamma\kappa\nu}}. \tag{27}$$

Family 6. When $\lambda^2 - 4\mu = 0$, $\lambda \neq 0$ and $\mu \neq 0$, then

$$u(x, y, t) = -\frac{\mathrm{i}e^{\mathrm{i}(x\kappa - t\nu + y\omega)}\sqrt{\nu + c(\kappa - 2\omega)}}{(1 - ct + x + y + \epsilon)\sqrt{-\gamma\kappa\nu}}. \tag{28}$$

Family 7. When $\lambda^2 - 4\mu = 0$, $\lambda = 0$ and $\mu = 0$,

$$u(x, y, t) = 0. \tag{29}$$

Case 4. When $a_0 = -\frac{\mathrm{i}\lambda\sqrt{c\kappa + \nu - 2c\omega}}{\sqrt{2c\gamma\lambda^2 - 8c\gamma\mu - 4\gamma\kappa\nu}}$,$a_1 = 0$, $b_1 = -\frac{2\mathrm{i}\sqrt{c\kappa + \nu - 2c\omega}}{\sqrt{2c\gamma\lambda^2 - 8c\gamma\mu - 4\gamma\kappa\nu}}$ and $\alpha = \frac{\lambda^2 - 4\mu + 2\kappa(\kappa - 2\omega)}{(c\kappa - \nu)(c(\lambda^2 - 4\mu) - 2\kappa\nu)}$ we get the following family solution:

Family 1. When $\lambda^2 - 4\mu > 0$, $\lambda \neq 0$ and $\mu \neq 0$, then

$$u(x, y, t) = -\frac{\mathrm{i}e^{\mathrm{i}(x\kappa - t\nu + y\omega)}\sqrt{\nu + c(\kappa - 2\omega)}\left(\lambda^2 - 4\mu + \lambda\sqrt{\lambda^2 - 4\mu}\tanh\left(\frac{1}{2}(-ct + x + y + \epsilon)\sqrt{\lambda^2 - 4\mu}\right)\right)}{\sqrt{2}\sqrt{\gamma(c(\lambda^2 - 4\mu) - 2\kappa\nu)}\left(\lambda + \sqrt{\lambda^2 - 4\mu}\tanh\left(\frac{1}{2}(-ct + x + y + \epsilon)\sqrt{\lambda^2 - 4\mu}\right)\right)}. \tag{30}$$

Family 2. When $\lambda^2 - 4\mu < 0$, $\lambda \neq 0$ and $\mu \neq 0$, then

$$u(x, y, t) = -\frac{\mathrm{i}e^{\mathrm{i}(x\kappa - t\nu + y\omega)}\sqrt{\nu + c(\kappa - 2\omega)}\left(\lambda - \frac{4\mu}{\lambda - \sqrt{-\lambda^2 + 4\mu}\tan\left[\frac{1}{2}(-ct + x + y + \epsilon)\sqrt{-\lambda^2 + 4\mu}\right]}\right)}{\sqrt{2}\sqrt{\gamma(c(\lambda^2 - 4\mu) - 2\kappa\nu)}} \tag{31}$$

Family 3. When $\lambda = 0$ and $\mu < 0$, then

$$u(x, y, t) = -\frac{\mathrm{i}e^{\mathrm{i}(x\kappa - t\nu + y\omega)}\sqrt{-\mu}\sqrt{\nu + c(\kappa - 2\omega)}\tanh((-ct + x + y + \epsilon)\sqrt{-\mu})}{\sqrt{-\gamma(2c\mu + \kappa\nu)}}. \tag{32}$$

Family 4. When $\lambda = 0$ and $\mu > 0$, then

$$u(x, y, t) = -\frac{\mathrm{i}e^{\mathrm{i}(x\kappa - t\nu + y\omega)}\sqrt{\mu}\sqrt{\nu + c(\kappa - 2\omega)}\tan((-ct + x + y + \epsilon)\sqrt{\mu})}{\sqrt{-\gamma(2c\mu + \kappa\nu)}}. \tag{33}$$

Family 5. When $\lambda^2 - 4\mu > 0$ and $\mu = 0$, then

$$u(x, y, t) = -\frac{\mathrm{i}e^{\mathrm{i}(x\kappa - t\nu + y\omega)}\lambda\sqrt{\nu + c(\kappa - 2\omega)}\coth\left(\frac{1}{2}(-ct + x + y + \epsilon)\lambda\right)}{\sqrt{2}\sqrt{\gamma(c\lambda^2 - 2\kappa\nu)}}. \tag{34}$$

Family 6. When $\lambda^2 - 4\mu = 0$, $\lambda \neq 0$ and $\mu \neq 0$, then

$$u(x, y, t) = \frac{\mathrm{i}e^{\mathrm{i}(x\kappa - t\nu + y\omega)}\sqrt{\nu + c(\kappa - 2\omega)}}{(-ct + x + y + \epsilon)\sqrt{-\gamma\kappa\nu}}. \tag{35}$$

Family 7. When $\lambda^2 - 4\mu = 0$, $\lambda = 0$ and $\mu = 0$, then

$$u(x, y, t) = -\frac{\mathrm{i}e^{\mathrm{i}(x\kappa - t\nu + y\omega)}\sqrt{\nu + c(\kappa - 2\omega)}}{(-ct + x + y + \epsilon)\sqrt{-\gamma\kappa\nu}} \tag{36}$$

3. Instability modulation

In this section, we analyze the modulation instability (MI) of the stationary solutions of equation (6) by utilizing the virtue of linear stability analysis [50–52]. The MI may consist of the exponential growth of small disturbances in the amplitude or optical wave phase. It is essential to observe the MI in the nonlinear physics of the wave. Assume that equation (6) have the following stationary solutions [53, 54]:

$$u(x, y, t) = ae^{\mathrm{i}\psi t}, \tag{37}$$

where a is arbitrary real constants. Inserting equation (37) into equation (6), we get $\psi = \sqrt{\frac{2a^2\gamma}{\alpha}}$. Suppose that the perturbed stationary solution is given by:

$$u(x, y, t) = (a + \varepsilon U(x, y, t))e^{\mathrm{i}\sqrt{\frac{2a^2\gamma}{\alpha}}t}, \tag{38}$$

here $U(x, y, t)$ is a complex function. Using equations (38) and (6), the outcomes satisfy the following linear equations

$$a\gamma(U + U^*) + \alpha\, U_{tt} + 2\mathrm{i}\, U_y + \beta\, U_{xx} = 0. \tag{39}$$

Where U^* is the conjugate function. therefore, equation (39) can be defined as

$$U(x, y, t) = u_1 e^{\mathrm{i}(Mx + Ny - Wt)} + u_2 e^{-\mathrm{i}(Mx + Ny - Wt)}, \tag{40}$$

where W denotes the complex frequency, M, N are real disturbance wave-numbers, and u_1, u_2 are the coefficients of the linear combination. Using equation (40) and putting into equation (39), we get the following homogeneous equations

$$\begin{aligned}(a^2\gamma - 2N - W^2\alpha - M^2\beta)U_1 + \gamma a^2 U_2 = 0,\\ \gamma a^2 U_1 + (-W^2\alpha + M^2\beta + a^2\gamma + 2N)U_2 = 0.\end{aligned} \tag{41}$$

Evaluating the determinant, we get the following relationship:

$$-4N^2 + W^4\alpha^2 - 4M^2N\beta - M^4\beta^2 - 2a^2W^2\alpha\gamma = 0. \tag{42}$$

Due to equation (42), we can discuss the following cases of the MI [53, 54] for equation (6) as follows:
Case 1. If

$$M = \mp\sqrt{-\frac{2N}{\beta} - \frac{\sqrt{W^2\alpha\beta^2(W^2\alpha - 2a^2\gamma)}}{\beta^2}}, \tag{43}$$

we observe that the MI of the equation (6) occur if satisfy the following inequalities

$$W^2\alpha\beta^2(W^2\alpha - 2a^2\gamma) < 0$$

or

$$-\frac{2N}{\beta} - \frac{\sqrt{W^2\alpha\beta^2(W^2\alpha - 2a^2\gamma)}}{\beta^2} < 0,$$

when $\beta \neq 0$.
Case 2. If

$$M = \mp\sqrt{-\frac{2N}{\beta} + \frac{\sqrt{W^2\alpha\beta^2(W^2\alpha - 2a^2\gamma)}}{\beta^2}}, \tag{44}$$

the MI of the equation (6) occur if satisfy the following inequalities

$$W^2\alpha\beta^2(W^2\alpha - 2a^2\gamma) < 0$$

or

$$-\frac{2N}{\beta} + \frac{\sqrt{W^2\alpha\beta^2(W^2\alpha - 2a^2\gamma)}}{\beta^2} < 0,$$

when $\beta \neq 0$. Now we investigate MI gain spectrum as

$$g(W) = 2\,\mathrm{Im}(M) = 2\sqrt{-\frac{2N}{\beta} - \frac{\sqrt{W^2\alpha\beta^2(W^2\alpha - 2a^2\gamma)}}{\beta^2}}, \tag{45}$$

$$g(W) = 2\,\mathrm{Im}(M) = 2\sqrt{-\frac{2N}{\beta} + \frac{\sqrt{W^2\alpha\beta^2(W^2\alpha - 2a^2\gamma)}}{\beta^2}}, \tag{46}$$

which can be observe that gain the MI gain is significantly affected by and that represents dispersion, diffraction of equation (6).

4. Conclusion

In this paper, we used the modified auxiliary expansion method to construct some novel soliton solutions of the (2+1)-dimension paraxial nonlinear Schrödinger equation. We presented a new solution in terms of hyperbolic, trigonometric and exponential functions. The instability modulation of the paraxial wave equation is also presented and analyzed in two cases. According to MI, the MI gain spectrum in the normal-GVD and anomalous-GVD for both cases are studied and illustrated graphically. The affection of all parameters are also illustrated. All our solutions are new, satisfy main paraxial wave equation and might be useful and applicable in the optical fiber industry. Figure 1 and figure 3 represent the dark solution, figure 2 and figure 4 are dark-singular solutionand figure 5 is a singular solution of equation (6). After considering simulations, figure 1 and figure 3 represent the dark solution, figure 2 and figure (4) are dark-singular solution and figure 5 is a singular solution of equation (6).

From figure 6, we conclude that the MI gain spectrum in the normal-GVD regime is increasing via increasing the values of Kerr nonlinearity (γ), real amplitude (a) and real disturbance wave-number (N) while we observe contrary affection of diffraction values β. Also from figure 7, the MI gain spectrum in the anomalous-GVD is decreased by increasing the values of diffraction, real amplitude, and real

disturbance wave-number while we see opposite direction of affection for values of real disturbance wave-number.

From figure 8, the MI gain spectrum in the normal-GVD is decreased by increasing the values of diffraction, real amplitude, and real disturbance wave-number while we see opposite direction of affection for values of real disturbance wave-number, which is the same effect in the anomals-GVD at equation (45). In another figure, we observe from figure 9 the same affection in the normal-GVD in equation (45). So, from these, we conclude that the normal-GVD obtained from equation (45) have the same characteristics of anomalous-GVD obtained from equation (46), Also anomalous-GVD obtained from equation (45) is the same as normal-GVD obtained from equation (46).

References

[1] Ali K, Rizvi S T R, Nawaz B and Younis M 2019 Optical solitons for paraxial wave equation in Kerr media *Mod. Phys. Lett.* B **33** 1950020

[2] Benjamin T B and Feir J E 1967 The disintegration of wave trains on deep water: I. Theory *J. Fluid Mech.* **27** 417–30

[3] Hammouch Z and Guedda M 2013 Existence and non-uniqueness of solution for a mixed convection flow through a porous medium *J. Appl. Math. Inf.* **31** 631–42

[4] Ali K K, Ismael H F, Mahmood B A and Yousif M A 2017 MHD Casson fluid with heat transfer in a liquid film over unsteady stretching plate *Int. J. Adv. Appl. Sci.* **4** 55–8

[5] Amkadni M, Azzouzi A and Hammouch Z 2008 On the exact solutions of laminar MHD flow over a stretching flat plate *Commun. Nonlinear Sci. Numer. Simul.* **13** 359–68

[6] Ismael H F 2017 Carreau–Casson fluids flow and heat transfer over stretching plate with internal heat source/sink and radiation *Int. J. Adv. Appl. Sci. J.* **6** 81–6

[7] Yokus A and Bulut H 2018 Numerical simulation of KdV equation by finite difference method *Indian J. Phys.* **92** 1571–5

[8] Yokus A, Sulaiman T A, Gulluoglu M T and Bulut H 2018 Stability analysis, numerical and exact solutions of the (1+ 1)-dimensional NDMBBM equation *ITM Web of Conf.* **22** 1064

[9] Yousif M A, Mahmood B A, Ali K K and Ismael H F 2016 Numerical simulation using the homotopy perturbation method for a thin liquid film over an unsteady stretching sheet *Int. J. Pure Appl. Math.* **107** 289–300

[10] Baskonus H M and Bulut H 2015 On the numerical solutions of some fractional ordinary differential equations by fractional Adams–Bashforth–Moulton method *Open Math.* **13** 547–56

[11] Ismael H F and Ali K K 2017 MHD casson flow over an unsteady stretching sheet *Adv. Appl. Fluid Mech.* **20** 533–41

[12] Biswas A, Yıldırım Y, Yaşar E and Alqahtani R T 2018 Optical solitons for Lakshmanan–Porsezian–Daniel model with dual-dispersion by trial equation method *Optik* **168** 432–9

[13] Wang Y-Y, Dai C-Q, Zhou G-Q, Fan Y and Chen L 2017 Rogue wave and combined breather with repeatedly excited behaviors in the dispersion/diffraction decreasing medium *Nonlinear Dyn.* **87** 67–73

[14] Zhao Z 2019 Bäcklund transformations, rational solutions and soliton-cnoidal wave solutions of the modified Kadomtsev–Petviashvili equation *Appl. Math. Lett.* **89** 103–10

[15] Daddy Moleleki L, Motsepa T and Masood Khalique C 2019 Solutions and conservation laws of a generalized second extended (3+1)-dimensional Jimbo–Miwa equation *Appl. Math. Nonlinear Sci.* **3** 459–74

[16] Rezazadeh H, Mirzazadeh M, Mirhosseini-Alizamini S M, Neirameh A, Eslami M and Zhou Q 2018 Optical solitons of Lakshmanan–Porsezian–Daniel model with a couple of nonlinearities *Optik* **164** 414–23

[17] Khalique C M and Mhlanga I E 2018 Travelling waves and conservation laws of a (2+1)-dimensional coupling system with Korteweg–de Vries equation *Appl. Math. Nonlinear Sci.* **3** 241–54

[18] Manafian J, Foroutan M and Guzali A 2017 Applications of the ETEM for obtaining optical soliton solutions for the Lakshmanan–Porsezian–Daniel model *Eur. Phys. J. Plus* **132** 494

[19] Zhao Z, He L and Gao Y 2019 Rogue wave and multiple lump solutions of the (2+1)-dimensional Benjamin-Ono equation in fluid mechanics *Complexity* **2019** 1–18

[20] Zhao Z and He L 2019 Multiple lump solutions of the (3+1)-dimensional potential Yu–Toda–Sasa–Fukuyama equation *Appl. Math. Lett.* **95** 114–21

[21] Bulut H, Sulaiman T A and Baskonus H M 2018 Optical solitons to the resonant nonlinear Schrödinger equation with both spatio-temporal and inter-modal dispersions under Kerr law nonlinearity *Optik* **163** 49–55

[22] Bulut H, Sulaiman T A and Baskonus H M 2018 Dark, bright and other soliton solutions to the Heisenberg ferromagnetic spin chain equation *Superlattices Microstruct.* **123** 12–19

[23] Baskonus H M, Yel G and Bulut H 2017 Novel wave surfaces to the fractional Zakharov–Kuznetsov–Benjamin–Bona–Mahony equation *AIP Conf. Proc.* **1863** 560084

[24] Yokus A, Sulaiman T A and Bulut H 2018 On the analytical and numerical solutions of the Benjamin–Bona–Mahony equation *Opt. Quantum Electron.* **50** 31

[25] Baskonus H M and Bulut H 2015 On the complex structures of Kundu–Eckhaus equation via improved Bernoulli sub-equation function method *Waves Random Complex Medium* **25** 720–8

[26] Biswas A, Kara A H, Alqahtani R T, Ullah M Z, Triki H and Belic M 2018 Conservation laws for optical solitons of Lakshmanan–Porsezian–Daniel model *Proc. Rom. Acad. Ser.* A **19** 39–44

[27] Javid A and Raza N 2018 Singular and dark optical solitons to the well posed Lakshmanan–Porsezian–Daniel model *Optik* **171** 120–9

[28] Biswas A *et al* 2018 Optical solitons with Lakshmanan–Porsezian–Daniel model using a couple of integration schemes *Optik* **158** 705–11

[29] Vega-Guzman J, Biswas A, Mahmood M F, Zhou Q, Moshokoa S P and Belic M 2018 Optical solitons with polarization mode dispersion for Lakshmanan–Porsezian–Daniel model by the method of undetermined coefficients *Optik* **171** 114–9

[30] Manafian J, Lakestani M and Bekir A 2016 Study of the analytical treatment of the (2+1)-dimensional Zoomeron, the duffing and the SRLW equations via a new analytical approach *Int. J. Appl. Comput. Math.* **2** 243–68

[31] Biswas A, Yildirim Y, Yasar E, Zhou Q, Alshomrani A S, Moshokoa S P and Belic S P 2018 Dispersive optical solitons with differential group delay by a couple of integration schemes *Optik* **162** 108–20

[32] Jawad A J M, Abu-AlShaeer M J, Biswas A, Zhou Q, Moshokoa S and Belic M 2018 Optical solitons to Lakshmanan–Porsezian–Daniel model for three nonlinear forms *Optik* **160** 197–202

[33] Wang Y-Y, Zhang Y-P and Dai C-Q 2016 Re-study on localized structures based on variable separation solutions from the modified tanh-function method *Nonlinear Dyn.* **83** 1331–9

[34] Yépez-Martínez H and Gómez-Aguilar J F 2019 M-derivative applied to the soliton solutions for the Lakshmanan–Porsezian–Daniel equation with dual-dispersion for optical fibers *Opt. Quantum Electron.* **51** 31

[35] Hammouch Z, Mekkaoui T and Sadki H 2017 Similarity solutions of a steady MHD flow over a semi-infinite surface *Math. Eng. Sci. Aerosp.* **8** 109–17
[36] Dewasurendra M and Vajravelu K 2018 On the method of inverse mapping for solutions of coupled systems of nonlinear differential equations arising in nanofluid flow *Heat Mass Transfer, Appl. Math. Nonlinear Sci.* **3** 1–14
[37] Ding D-J, Jin D-Q and Dai C-Q 2017 Analytical solutions of differential-difference sine-Gordon equation *Therm. Sci.* **21** 1701–5
[38] Dai C-Q, Fan Y and Wang Y-Y 2019 Three-dimensional optical solitons formed by the balance between different-order nonlinearities and high-order dispersion/diffraction in parity-time symmetric potentials *Nonlinear Dyn.* **98** 1–11
[39] Wang Y-Y, Chen L, Dai C-Q, Zheng J and Fan Y 2017 Exact vector multipole and vortex solitons in the media with spatially modulated cubic-quintic nonlinearity *Nonlinear Dyn.* **90** 1269–75
[40] Dai C-Q, Zhou G-Q, Chen R-P, Lai X-J and Zheng J 2017 Vector multipole and vortex solitons in two-dimensional Kerr media *Nonlinear Dyn.* **88** 2629–35
[41] Heydari M H, Hooshmandasl M R, Maalek Ghaini F M and Cattani C 2014 A computational method for solving stochastic ItÔ–Volterra integral equations based on stochastic operational matrix for generalized hat basis functions *J. Comput. Phys.* **270** 402–15
[42] Cattani C 2003 Multiscale analysis of wave propagation in composite materials *Math. Model. Anal.* **8** 267–82
[43] Zhao Z and Han B 2019 Lump solutions of a (3+1)-dimensional B-type KP equation and its dimensionally reduced equations *Anal. Math. Phys.* **9** 119–30
[44] Osman M S and Ghanbari B 2018 New optical solitary wave solutions of Fokas-Lenells equation in presence of perturbation terms by a novel approach *Optik* **175** 328–33
[45] Ghanbari B 2019 Abundant soliton solutions for the Hirota-Maccari equation via the generalized exponential rational function method *Mod. Phys. Lett.* B **33** 1950106
[46] Cattani C 2003 Harmonic wavelet solutions of the Schrodinger equation *Int. J. Fluid Mech. Res.* **30** 1–10
[47] Pavlova L M, Pashinkin A S, Gaev D S and Pak A S 2006 The heat capacity of cadmium telluride at medium and high temperatures *High Temp.* **44** 843–51
[48] Cattani C, Chen S and Aldashev G 2012 Information and modeling in complexity *Math. Probl. Eng.* **2012** 1-2
[49] Cattani C, Sulaiman T A, Baskonus H M and Bulut H 2018 Solitons in an inhomogeneous Murnaghanas rod *Eur. Phys. J. Plus* **133** 228
[50] Cazenave T and Lions P-L 1982 Orbital stability of standing waves for some nonlinear Schrödinger equations *Commun. Math. Phys.* **85** 549–61
[51] Feng B and Zhang H 2018 Stability of standing waves for the fractional Schrödinger–Choquard equation *Comput. Math. with Appl.* **75** 2499–507
[52] Feng B and Zhang H 2018 Stability of standing waves for the fractional Schrödinger–Hartree equation *J. Math. Anal. Appl.* **460** 352–64
[53] Cazenave T 2003 *Semilinear Schrodinger Equations* 10 (Providence, RI: American Mathematical Society) (https://doi.org/10.1090/cln/010)
[54] Feng B, Chen R and Wang Q 2019 Instability of standing waves for the nonlinear Schrödinger–Poisson equation in the L^2-critical case *J. Dyn. Differ. Equations* **0** 1–14